

Original article

Predicting adsorbed gas capacity of deep shales under high temperature and pressure: Experiments and modeling

Shangwen Zhou^{1,2}, Hongyan Wang^{1,2}^{*}, Bobo Li³, Shuangshuang Li⁴, Kamy Sepehrnoori⁵, Jianchao Cai⁶

¹PetroChina Research Institute of Petroleum Exploration & Development, Beijing 100083, P. R. China

²National Energy Shale Gas R&D (Experiment) Center, Langfang 065007, P. R. China

³College of Mining, Guizhou University, Guiyang 550025, P. R. China

⁴Institute of Geophysics and Geomatics, China University of Geosciences, Wuhan 430074, P. R. China

⁵Hildebrand Department of Petroleum and Geosystems Engineering, The University of Texas at Austin, Austin 78712, USA

⁶State Key Laboratory of Petroleum Resources and Prospecting, China University of Petroleum, Beijing 102249, P. R. China

Keywords:

Deep shale
shale gas
adsorbed gas
prediction method
model building

Cited as:

Zhou, S., Wang, H., Li, B., Li, S., Sepehrnoori, K., Cai, J. Predicting adsorbed gas capacity of deep shales under high temperature and pressure: Experiments and modeling. *Advances in Geo-Energy Research*, 2022, 6(6): 482-491.

<https://doi.org/10.46690/ager.2022.06.05>

Abstract:

Temperature and pressure conditions of deep shale are beyond experiment range, and the amount of adsorbed gas is difficult to determine. To predict the adsorbed gas content of deep shales under formation conditions, isothermal adsorption experiments and model building were conducted on shale samples from Longmaxi Formation in China. A temperature-dependent adsorption model based on the Langmuir equation is proposed, which can be well-fitted by observed isotherms with a high correlation coefficient. Based on the fitted parameters at 303.15 K, the isothermal adsorption curves at 333.15 K, 363.15 K, and 393.15 K are predicted, showing a good agreement with experimental curves available. Compared with previous prediction methods, the biggest advantage of the proposed method is that it can be carried out only based on one-time isothermal adsorption experiment. Based on the predictions, the downward trend of the excess adsorption curves will slow down under high temperature and pressure conditions, and when the pressure reaches a certain level (> 80 MPa), the temperature has little effect on the excess adsorption capacity. While for absolute adsorption, the gas adsorption reaches saturation much slowly at high temperature, it can also reach saturation under formation pressure. Under the burial depth of marine shale, temperature plays a major role in controlling the adsorbed gas, resulting in the decrease of adsorbed gas content in deep shale, and its ratio will further decrease as the depth increases.

1. Introduction

Shale gas has basically achieved industrial development in China, and the output in 2021 has reached 23 billion cubic meters, basically all of which comes from the lower Silurian marine shale gas in the Sichuan Basin (Ma et al., 2020; Hartman et al., 2021; Zou et al., 2021). The depth of shale gas that has been developed so far is mainly shallower than 3,500 m, and the deep shale gas (3,500~4,500 m) is an important replacement area in the future (Dong et al., 2018; Zhang et al., 2019; Cai et al., 2021), which is of great

significance for the sustainable development of natural gas production in China (Ma et al., 2021). Due to the existence of a large amount of organic matter and micropores in shale, in addition to the existence of free gas, some gases also exist in the form of adsorbed gas (Pan et al., 2015; Wu et al., 2015; Yu et al., 2016). At present, the proportion of adsorbed gas in the developed shale gas fields in China is about 30%~70% (Curtis, 2002; Mengal et al., 2011; Li et al., 2022), and the gas volume of this part cannot be ignored. Therefore, the accurate evaluation of adsorbed gas capacity of deep shale has

important implications for determining subsurface gas reserves and designing development plans.

For the shale nanopore-gas system, many studies have been conducted about the shale gas adsorption characteristics, models and mechanisms (Ambrose et al., 2012), and the following understandings have been formed: (1) shale gas adsorption belongs to supercritical adsorption, and its isothermal adsorption curves will have a maximum value, generally when the pressure is around 10 MPa, which is caused by the different trends of adsorbed-phase density and gas-phase density with pressure (Zhou et al., 2018); (2) shale gas adsorption belongs to physical adsorption. Methane is generally adsorbed on the pore surface in the form of single-layer or double-layer adsorption under the force of the pore wall according to the surface coverage theory (Xiong et al., 2017; Zhou et al., 2018; Pang et al., 2019). Some scholars also believe that the micropore-filling is the dominant adsorption mechanism, especially for shales rich in micropores (Ross and Bustin, 2009; Rexer et al., 2014; Yang et al., 2022); (3) shale gas adsorption is mainly controlled by the specific surface area (SSA) of pores. The larger the SSA, the greater the adsorption capacity (Chalmers et al., 2012; Yu et al., 2016a; Xiang et al., 2019). Due to the large SSA of shale, about 10~30 m²/g (Zhou et al., 2019), it has a certain adsorption capacity; (4) affected by the adsorption force, under a certain pressure, methane molecules are preferentially adsorbed in the micropores (< 2 nm), and the micropores are the main storage space for the adsorbed gas (Zhu et al., 2020).

In order to describe the adsorption behavior and clarify the maximum adsorption capacity of gas in shale, an adsorption model is critically needed. Based on different adsorption theories, such as monolayer adsorption, multilayer adsorption and micropore filling, many different adsorption models have been established in previous studies. These models mainly include Langmuir model (Zhang et al., 2012; Xue et al., 2013; Wang et al., 2016; Xiong et al., 2017), improved Langmuir-Freundlich (L-F) model (Wang et al., 2016), Brunauer-Emmett-Teller (BET) model (Brunauer et al., 1938; Sing, 1998), simplified local density (SLD) model (Bharath et al., 2020), Ono-Kondo model (Ono and Kondo, 1960; Donohue and Aranovich, 1998; Pang et al., 2019), supercritical Dubinin-Radshkevich (SDR) model (Huston and Yang, 1938; Sakurovs et al., 1998), etc. All the models were well applied in shale gas adsorption curve fitting, adsorption capacity determination and thermodynamic analysis (Xue et al., 2013). However, these models are only suitable for the fitting of gas adsorption curves under a certain temperature condition, and cannot be used to predict the adsorption curves under unknown temperature conditions.

Few studies have proposed methods for the prediction of the adsorption curves under different temperature conditions. One method is to fit the isotherms based on the Polanyi adsorption potential theory (Polanyi, 1963; Dubinin and Stoeckli, 1980; Liu et al., 2022). The adsorption data at a known temperature can be fitted to obtain an adsorption characteristic curve, thereby predicting the adsorption curve of an unknown temperature based on the characteristic curve. Another method is based on the Clausius-Clapeyron isosteric heat of adsorption with the relationship between equilibrium

pressure and temperature (Gasparik et al., 2014; Li et al., 2021). This method takes advantage of the fact that the adsorption heat does not change with temperature, and obtains the logarithm of pressure and temperature through known adsorption data, thereby predicting the adsorption curve for an unknown temperature. However, there is no strict theoretical derivation and physical meaning during the creation of the two methods, and in order to ensure fitting accuracy, it is generally necessary to know two or three adsorption curves at multiple temperatures (Gasparik et al., 2013). Using only one isotherm adsorption curve to predict the adsorption curves under other temperatures is still rarely reported. Due to the low adsorption capacity and long adsorption equilibrium time of shale, the isothermal adsorption experiment of a shale sample at one temperature condition generally takes 3~4 days. Therefore, it will cost a lot of material resources and time to carry out the adsorption experiment at multiple temperature conditions for each sample. Therefore, it is of great significance to predict the real adsorption capacity of shale by carrying out only one-time adsorption experiment.

In addition, the commonly used isothermal adsorption equipment is also limited by temperature and pressure. For gravimetric adsorption apparatus, the highest temperature and pressure are about 150 °C and 35 MPa, respectively (Chen et al., 2018; Wu et al., 2019). Whereas for the volumetric adsorption apparatus, the highest temperature and pressure are about 177 °C and 69 MPa, respectively (Duan et al., 2018). For medium-shallow shale, this temperature and pressure condition is applicable. But for deep marine shales in China, its geothermal gradient and pressure gradient can reach 2.8 °C/100 m and 2.2 MPa/100 m, so at a depth of about 4,000 m, its formation temperature and pressure can reach 130 °C and 88 MPa, which will reach or exceed the limits of the experimental device. In addition, under the conditions of ultra-high temperature and pressure, the performance and stability of the equipment will also be affected to a certain extent, resulting in a decrease in the accuracy of testing the adsorption capacity. Therefore, accurately obtaining or predicting the adsorption curve of deep shale has become a key problem that needs to be solved urgently.

This study aims at establishing a temperature-dependent adsorption model, and use the adsorption model to fit the experimental adsorption curve and predict the adsorption curve under unknown temperature conditions. Model applicability is analyzed by comparison with the predicted with experimental results, and finally the real adsorption gas content and change law of deep shale is obtained, which will provide an important basis for gas-bearing evaluation and reserves calculation under deep shale formation conditions.

2. Material and method

2.1 Samples

The samples were collected from the Lower Silurian Longmaxi Formation in southern Sichuan Basin, which is the main production layer of shale gas in China (Table 1). During the late Ordovician Wufeng period to the Early Silurian Longmaxi period, the Sichuan Basin was a deep-water shelf sandwiched

by uplifts (Fig. 1). Black shale with a thickness of 60 m was deposited in a low-energy, under compensated and anoxic environment (Ma et al., 2020). From the Middle Permian to the early Cretaceous, Longmaxi Formation continued to be strongly buried to a depth of more than 6,000 m, and the organic matter reached an over mature stage, forming an unconventional dry gas reservoir by self-generation and self-storage. Since the late Cretaceous, this set of strata has experienced multi-stage uplift and surface erosion (Zhang et al., 2019). At present, the buried depth of shale gas in Longmaxi formation is generally between 2,500~5,500 m (Ma et al., 2020). The depth of the deep shale referred to is 3,500~4,500 m; it is called ultra-deep shale when it exceeds 4,500 m. For the selected samples, the organic maturity is 2.58% and 2.64%, indicating that it is in the over-mature stage, and the main gas product is dry gas. The kerogen composition of all the samples is dominated by sapropel and its kerogen belongs to type I.

2.2 Methane adsorption experiment

Isothermal methane adsorption experiments of shale samples were conducted by a gravimetric adsorption equipment (Fig. 2), featuring a high accuracy magnetic suspension balance of 10 μg . The maximum test temperature of this device is 150 $^{\circ}\text{C}$ and the maximum test pressure is 35 MPa (Zhou et al., 2018). The experimental temperature was set at 30, 60, 90, and 120 $^{\circ}\text{C}$ (303.15, 333.15, 363.15, and 393.15 K); the maximum pressure was set at 20 MPa, and the equilibrium time for every pressure point was set at 4 h. At a constant temperature condition, methane was adsorbed under different pressure and formed an inherent adsorbed phase over the surface of shale. The reading of the balance is the joint result of the weight of the sample barrel, sample, adsorbed methane, and the buoyancy of the sample barrel, sample, adsorbed phase. When considering the existence of the adsorbed phase volume, instead of directly measuring the actual adsorption capacity (absolute adsorption capacity) of methane, what isothermal adsorption experiment can actually measure is the excess adsorption capacity (Zhou et al., 2018), expressed as

$$m_{ex} = \Delta m - m_{sc} - m_s + (V_{sc} + V_s) \rho_g \quad (1)$$

where m_{ex} is the excess adsorption capacity of methane, g; Δm is the reading of the magnetic suspension balance, g; m_{sc} is the mass of the sample barrel, g; m_s is the mass of the sample, g; V_{sc} is the volume of the sample barrel, cm^3 ; V_s is the volume of the sample, cm^3 ; ρ_g is the density of the methane gas at different pressure points, g/cm^3 .

The absolute adsorption capacity can be transformed from the excess adsorption capacity by the following equation as

$$V_a = \frac{V_{ex}}{1 - \frac{\rho_g}{\rho_a}} \quad (2)$$

$$V_{ex} = \frac{m_{ex} \times 22.4 \times 1000}{m_s \times 16} \quad (3)$$

where V_{ex} is the excess adsorption capacity of methane, m^3/t ; V_a is the absolute adsorption capacity of methane, m^3/t ; ρ_a is the density of the adsorbed methane, g/cm^3 .

2.3 Temperature-dependent adsorption model

To describe the adsorption characteristics of methane in shale, the Langmuir adsorption model was commonly used in previous studies and it also has good applications (Wang et al., 2016). The Langmuir model was proposed based on monolayer adsorption theory, which is also applicable in the gas-shale system. The general expression of Langmuir model is (Guo et al., 2013)

$$V_a = V_L \frac{KP}{1 + KP} \quad (4)$$

where P is the experimental pressure, MPa; V_L is the maximum monolayer adsorption capacity, m^3/t ; K is an adsorption equilibrium constant, $K = 1/P_L$; P_L is the Langmuir pressure, MPa. If an isothermal adsorption curve can be got, these two key parameters (V_L , K) can be obtained by equation fitting. Conversely, if the two parameters (V_L , K) can be determined, predictions of the adsorption curves can then be made. Under different temperature conditions, both of V_L and K will be changed, and the following expressions can be used to reflect on the V_L and K at different temperatures (Cochran et al., 1985; Fianu et al., 2018).

$$V_L(T) = a_0 \exp\left(-\frac{e_0}{T}\right) \quad (5)$$

$$K(T) = A_0 \exp\left(-\frac{E_0}{RT}\right) \quad (6)$$

where a_0 , A_0 are pre-exponential coefficients; e_0 is a constant related to the temperature of the maximum adsorption capacity, K; E_0 is a constant related to adsorption heat, J/mol; R is a thermodynamic constant, 8.314 J/mol/K; T is the temperature, K. Therefore, by combining the Eqs. (4)-(6), a temperature-dependent adsorption model (Eq. (7)) can be established. In order to fit the experimental adsorption isotherm curve, based on Eq. (2), the excess adsorption capacity model can be obtained

$$V_a = a_0 \exp\left(-\frac{e_0}{T}\right) \frac{A_0 \exp\left(-\frac{E_0}{RT}\right) P}{1 + A_0 \exp\left(-\frac{E_0}{RT}\right) P} \quad (7)$$

$$V_{ex} = a_0 \exp\left(-\frac{e_0}{T}\right) \frac{A_0 \exp\left(-\frac{E_0}{RT}\right) P}{1 + A_0 \exp\left(-\frac{E_0}{RT}\right) P} \left(1 - \frac{\rho_g}{\rho_a}\right) \quad (8)$$

When using this model (Eq. (8)) to fit an isothermal curve under certain temperature by a nonlinear-fitting method, the parameter a_0 , A_0 , e_0 , E_0 , ρ_a can be got. Through literature survey and comparison, the range of these five parameters is determined: $0 < a_0 < 5 \text{ m}^3/\text{t}$; $-500 < e_0 < 0 \text{ K}$; $0.001 < A_0 < 0.01$; $-30,000 < E_0 < -10,000 \text{ J/mol}$; $0 < \rho_a < 1 \text{ g}/\text{cm}^3$. If these five parameters are assumed to be independent of temperature, they can be used to predict the adsorption curves at unknown temperatures. The adsorption curve at 303.15 K was fitted by the model, and then was used to predict the adsorption curves under 333.15, 363.15, and 393.15 K conditions, which were also tested. Residual error analysis was performed to assess the prediction accuracy of this model. The average relative error (δ) was used to evaluate the difference between the predicted

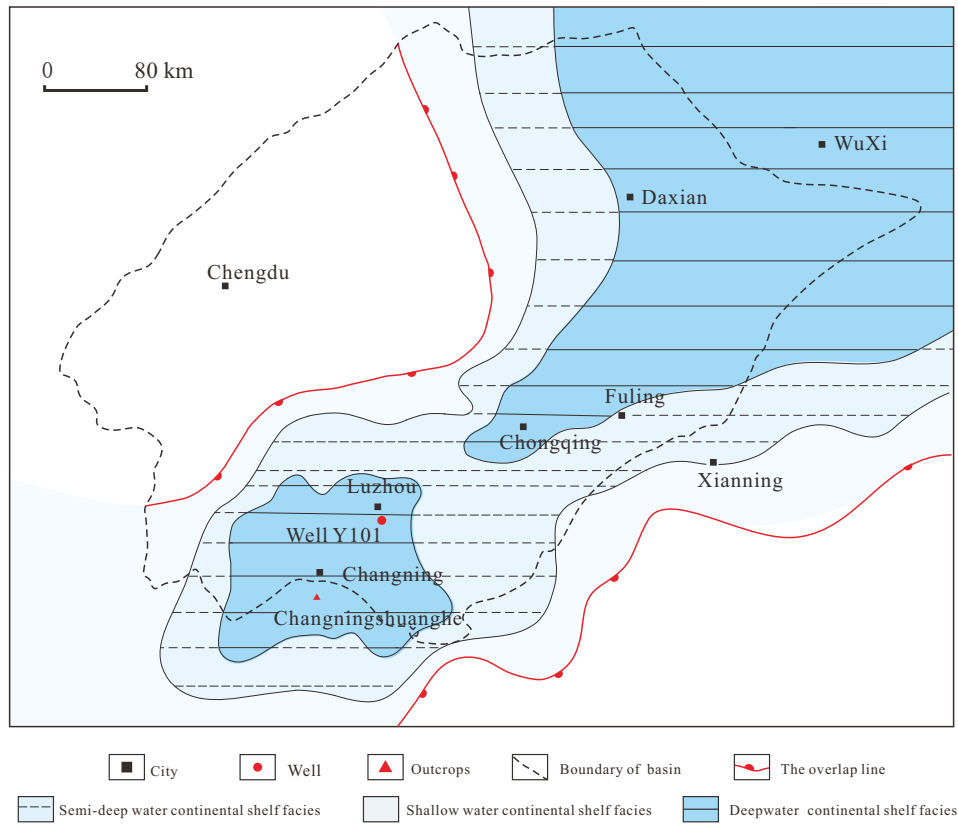


Fig. 1. Well sites, geographical locations of Well Y101.

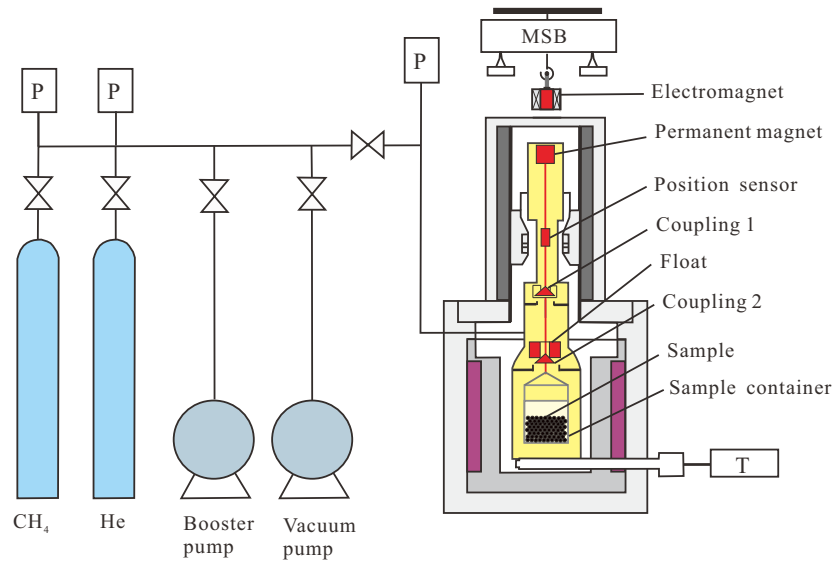


Fig. 2. The gravimetric isothermal adsorption instrument based on magnetic suspension balance.

Table 1. Basic data of the studied deep shale samples.

Sample	Depth (m)	TOC (%)	Quartz content (%)	Clay content (%)	R _o (%)
Y101-7	3880.55	3.39	47.7	18.6	2.58
Y101-8	3883.35	4.04	50.2	15.8	2.64

Notes: TOC is total organic carbon.

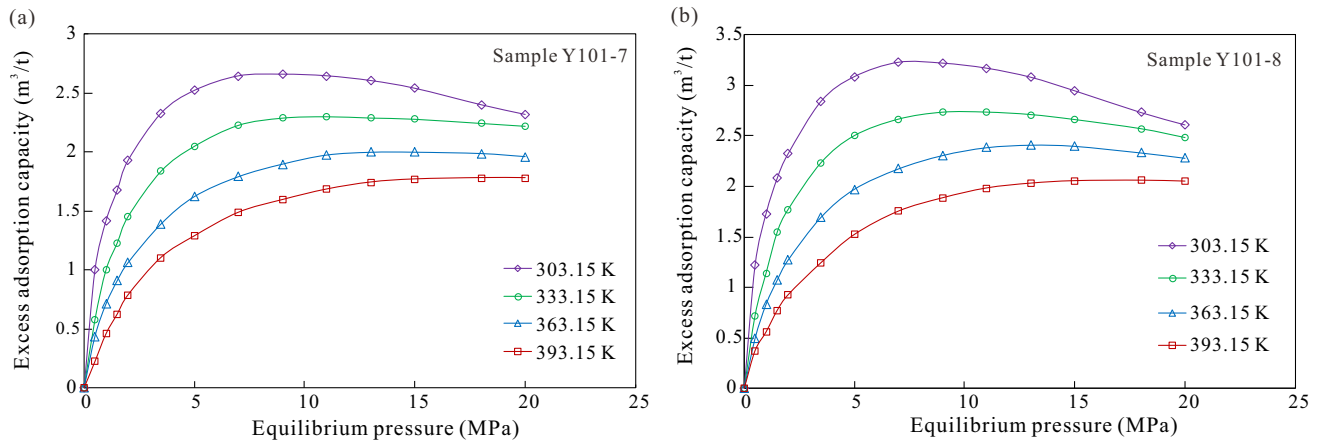


Fig. 3. The experimental methane isothermal adsorption curves of the two samples under different temperatures.

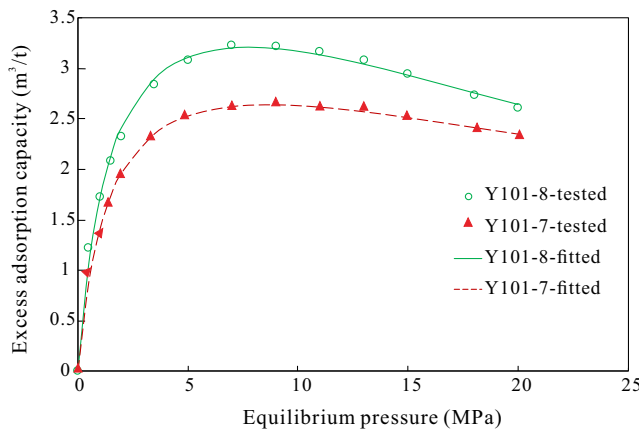


Fig. 4. The fitted results by the proposed temperature-dependent model under 303.15 K.

results and the experimental results, can be calculated by

$$\delta = \frac{1}{N} \sum_{i=1}^N \left(\frac{|V_{i,e} - V_{i,p}|}{V_{i,e}} \right) \quad (9)$$

where $V_{i,e}$ is the experimental adsorption capacity of methane, m^3/t ; $V_{i,p}$ is the predicted adsorption capacity of methane, m^3/t .

3. Results and discussion

3.1 Methane adsorption isotherms

The experimental isothermal adsorption curves of the deep shales are shown in Fig. 3 and the adsorption capacity at different pressures and temperatures is shown in Table 2. It can be seen that the adsorption capacity decreases with the increase of temperature. Since the adsorption process is exothermic, the increase of temperature will reduce the adsorption capacity of shale, which is consistent with previous understandings (Peter et al., 2008; Guo et al., 2013; Qin et al., 2022). Moreover, as the pressure increases, the adsorption capacity first increases and then decreases, reaching a maximum value at around 10 MPa at some temperature conditions. The decline trend of the adsorption curve under high pressure is caused by the density difference between gas-phase and adsorbed-phase of methane. Furthermore, as the temperature increases, this

downward trend becomes less and less obvious. This shows that under high temperature conditions, the speed of reaching adsorption saturation becomes slower. Under the maximum pressure of 20 MPa and maximum temperature of 393.15 K set in this study, the adsorption capacity has not yet reached saturation, and the adsorption curve has a certain upward trend under. This suggests that higher pressure is required for reaching adsorption saturation at high temperatures.

Overall, with the increase of temperature, the variation trend of the adsorption curves will be different, especially under high pressure. For deep shale buried at a depth of about 4000 m, the formation temperature and pressure have exceeded the limits of experimental apparatus, so the isotherms can only be predicted based on the existing experimental data.

3.2 Fitting results by the new model

The proposed model (Eq. (8)) was used to fit the isothermal curve under 303.15 K by a nonlinear-fitting method. In the fitting process, parameters a_0 , A_0 , e_0 , E_0 , and ρ_a were set as unknown constants of each sample. The fitting effect of the model is shown in Fig. 4. It can be seen that the fitting effect is very good, and the correlation coefficients are all above 0.99. The fitted parameters are shown in Table 3, for different samples, showing the values of these parameters show good consistency. The two samples are basically similar in pore structure. Mainly due to the difference of TOC, the adsorption capacity of the two samples shows a certain difference. The parameter a_0 of sample Y101-8 is slightly larger, and its saturated adsorption capacity will be larger.

According to Eqs. (5)-(6), we can the V_L and the P_L of the two samples can be obtained, and the calculated results are shown in Fig. 5. It can be seen that with the increase of temperature, the V_L decreases; on the contrary, the Langmuir pressure increases significantly. This suggests that the increase in temperature limits the final adsorption capacity of the shale, and even under the condition that the physical properties of the sample remain unchanged, the high temperature makes it more difficult for gas molecules to adsorb into the pores of shale. In addition, the increase in Langmuir pressure indicates that under high temperature conditions, the rate of shale reaching

Table 2. The adsorption capacity of sample Y101-7 under different pressures and temperatures.

303.15 K		333.15 K		363.15 K		393.15 K	
P (MPa)	V_{ex} (m ³ /t)						
0.000	0.000	0.000	0.000	0.000	0.000	0.000	0.000
0.491	0.999	0.495	0.578	0.493	0.436	0.498	0.223
0.993	1.416	0.995	1.002	0.991	0.712	1.003	0.458
1.503	1.676	1.502	1.230	1.496	0.909	1.503	0.625
1.993	1.929	1.998	1.454	1.994	1.062	2.001	0.788
3.492	2.329	3.491	1.840	3.494	1.391	3.494	1.105
4.992	2.522	4.992	2.050	4.994	1.621	4.999	1.287
6.994	2.645	6.995	2.230	6.997	1.791	6.994	1.487
9.001	2.660	8.996	2.291	8.993	1.898	8.995	1.595
10.997	2.646	10.996	2.303	10.998	1.975	10.997	1.684
13.004	2.606	12.997	2.291	12.994	1.999	13.001	1.744
14.997	2.541	15.001	2.281	14.995	1.999	14.996	1.770
18.005	2.401	18.005	2.246	18.000	1.988	17.998	1.781
20.006	2.318	20.005	2.221	19.999	1.962	20.001	1.780

Table 3. The fitted parameters by the proposed model under 303.15 K.

Sample	a_0 (m ³ /t)	e_0 (K)	A_0	E_0 (J/mol)	ρ_a (g/cm ³)	R^2	RSS
Y101-7	1.30933	-296.62	0.00272	-13961.28	0.55144	0.99523	0.0263
Y101-8	1.46444	-335.11	0.00274	-13782.81	0.42672	0.99387	0.0431

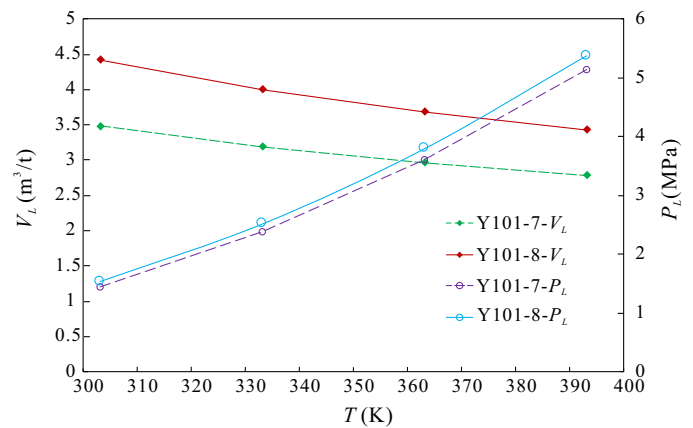
Notes: RSS is residual sum of squares, R^2 is fitting accuracy.

adsorption saturation becomes slower. Under low temperature conditions, only a pressure of about 1 MPa is needed to achieve half of the saturated adsorption capacity, while under high temperature conditions, this pressure value increases to about 5 MPa.

3.3 Predicting isotherms under high temperature

Based on the above parameters fitted at 303.15 K, the prediction under other experimental temperature conditions was carried out; the prediction results are compared with the experimental results to clarify the applicability of this method. The prediction and comparison results are shown in Fig. 6. It can be seen that the predicted isothermal adsorption curves were in good agreement with the experimental results under different temperatures. According to Eq. (9), average relative errors of sample Y101-7 under different temperature conditions are 1.82%, 2.72%, and 3.25%, respectively, showing a relatively high prediction accuracy.

Compared with the adsorption capacity prediction methods that have been reported so far (John et al., 2018), the significant advantage of proposed method in this study is that the prediction can be carried out only based on one-time isothermal adsorption experiment. For the commonly used

**Fig. 5.** Variation of V_L and P_L under different temperatures.

adsorption potential method (Dubinin and Stoeckli, 1980; Gasparik et al., 2014), it is critically needed to be experimentally determined the adsorption characteristic curve under three or more temperature conditions. Experiments with multiple temperature conditions for each sample would be time-consuming and labor-intensive. The proposed adsorption model and prediction method can be carried out on the basis of one-time experiment, which can achieve high accuracy and also save a lot of time and material resources.

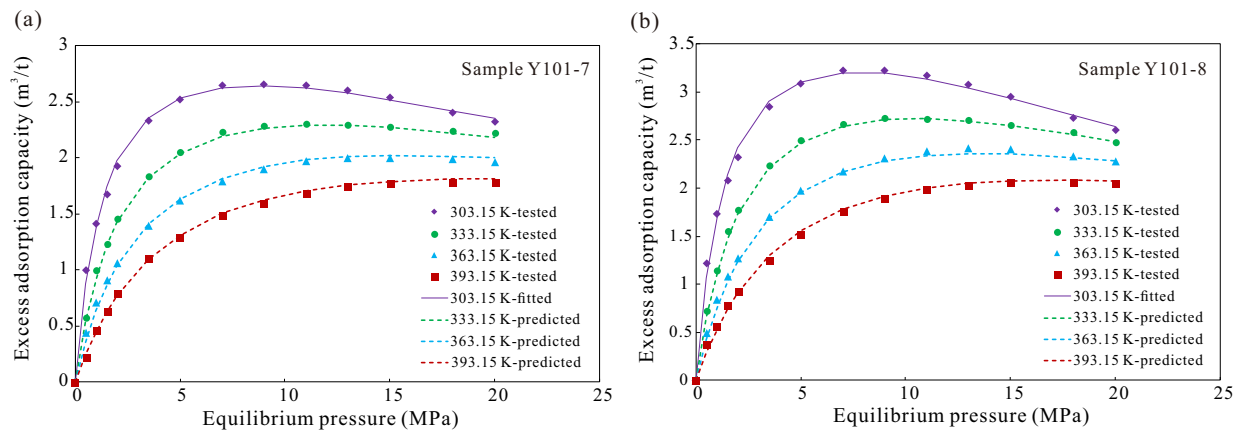


Fig. 6. The tested and predicted adsorption curves under different temperatures.

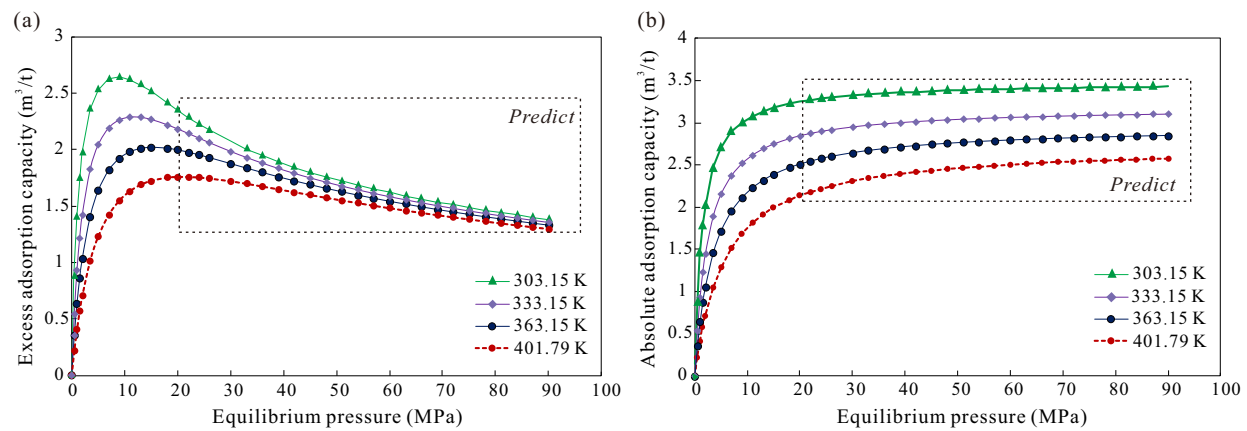


Fig. 7. The predicted isothermal adsorption curves under different temperatures.

3.4 Predicting isotherms under high pressure

On the basis of proving the applicability of the above model and prediction method, the adsorption curve prediction under high pressure far beyond the experimental pressure was carried out, as shown in Fig. 7. It can be seen that under high pressure, all the excess adsorption curves show an upward trend first and then a downward trend. It can be considered that the decline phenomenon not shown in the experimental test curve under the condition of 393.15 K (Fig. 2) is due to the insufficient experimental pressure. When the pressure is further increased, the curve will also show a significant decrease. In addition, under high temperature conditions, the downward trend of the curve will slow down. This is because the increase of temperature will lead to the decrease of methane gas density, and the increasing trend of methane gas density under high pressure will slow down. In the case of fixed adsorbed-phase methane density, the decline speed of the curves will slow down. Moreover, when the pressure reaches a certain degree (> 80 MPa), the difference of excess adsorption capacity of the same sample under different temperature conditions is very small, indicating that the temperature has little effect on the excess adsorption capacity under ultra-high pressure.

For the absolute adsorption curves, it can be seen that with the increase of pressure, the adsorption capacity first increases

rapidly, and then increases slowly until reaching saturation. And the saturated adsorption capacity can be reduced by about 25% from 303.15 K to 393.15 K. At low temperature, 90% of the saturated adsorption capacity can be reached with a low pressure (20 MPa); while at high temperature, when the pressure reaches 40 MPa, the absolute adsorption capacity still has a certain upward trend. For the deep shale (3,880 m) in the studied area, the temperature gradient is 2.8 °C/100 m, the pressure gradient is 2.2 MPa/100 m, so the formation temperature is 401.79 K (128.64 °C) and the formation pressure is 85.36 MPa. As can be seen from the Fig. 6, the adsorption capacity of deep shale has basically reached saturation, which is about 90% of the Langmuir volume.

3.5 Adsorbed gas characteristics of deep shales

For the deep marine shale in the southern Sichuan Basin, the formation temperature and pressure are significantly higher compared with those of the middle-shallow shale. Affected by the dual effects of high temperature and pressure, the characteristics of adsorbed gas in deep shale under formation conditions are complex. Based on the model and prediction method proposed in this study, the amount of adsorbed gas under the condition of deep shale formation is predicted, and the results are shown in Fig. 8. It can be seen that both the

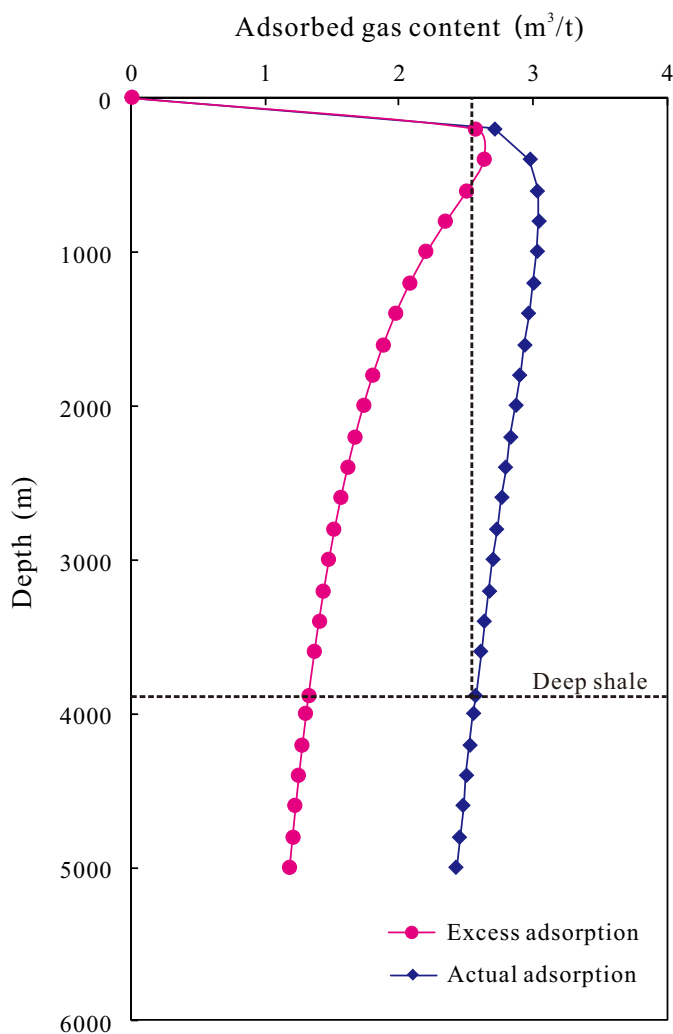


Fig. 8. Variation of excess and absolute adsorption content with depth.

excess and absolute adsorption amount show a trend of first increasing and then decreasing with the increase of depth. For the absolute adsorption amount, which represents the actual adsorption amount of shale, it reaches the maximum value at about 800 m, and thereafter, the adsorption amount continues to decrease. Since temperature and pressure have opposite controlling effects on the amount of adsorbed gas, this variation trend shows that with the increase of depth, the increase of pressure leads to the increase of the amount of adsorption, and the pressure is the main controlling factor. But with the further increase of depth, the increase of temperature leads to the decrease of the amount of adsorption, the temperature becomes the main controlling factor.

Therefore, under the condition of deep shale formation, the amount of adsorbed gas is low, but compared with the shale with depth of about 2,500 m, the adsorption amount is only reduced by about 10%. When the shale porosity and gas saturation are similar, the proportion of adsorbed gas in deep shale will be lower than that in middle-shallow shale. It is estimated that the proportion of adsorbed gas in deep shale is about 35%, and this value will further decrease as the depth increases.

It should be pointed out that the predictions made in this paper are based on the experimental results of dry shale samples, without considering the water content of shale. Under the actual formation conditions, shale contains a certain amount of water with a water saturation of about 30%, and it is mainly stored in the form of bound water. The existence of water will greatly reduce the adsorption capacity of shale (Li et al., 2020; 2021). Therefore, the actual adsorption capacity of deep shale under formation conditions will be further reduced compared with that predicted in this study, which has an important impact on the estimation of shale gas geological reserves, and will be further studied in the future work.

4. Conclusions

To predict the adsorbed gas content of deep shales under formation conditions, isothermal adsorption experiments and model building were conducted on shale samples from Longmaxi Formation. The adsorption isotherms under high temperature and pressure beyond the limit of the experiment were determined. The main conclusions are as follows:

- 1) A temperature-dependent adsorption model based on Langmuir equation was proposed, and the fitting effect of this model is very good with the correlation coefficients > 0.99 .
- 2) The predicted isothermal adsorption curves were in good agreement with the experimental results under 333.15, 363.15, and 393.15 K. Compared with previous prediction methods, the biggest advantage of the proposed method is that the prediction can be carried out only based on one-time isothermal adsorption experiment.
- 3) The downward trend of the excess adsorption curve will slow down under conditions of high temperature and pressure. When the pressure reaches a certain level (> 80 MPa), the temperature has little effect on the excess adsorption capacity, but the effect on the absolute adsorption capacity can be reduced by about 25%.
- 4) Under the burial depth of marine shale, temperature plays a major role in controlling the adsorbed gas content, resulting in the decrease of adsorbed gas content in deep shale, and its ratio will further decrease as the depth increases.

Acknowledgement

This study was funded by PetroChina Basic Technology Research Project (No. 2021DJ1905) and the Fundamental Research Funds for the Central Universities (No. 2462019YJRC011).

Conflict of interest

The authors declare no competing interest.

Open Access This article is distributed under the terms and conditions of the Creative Commons Attribution (CC BY-NC-ND) license, which permits unrestricted use, distribution, and reproduction in any medium, provided the original work is properly cited.

References

- Ambrose, R. J., Hartman, R. C., Diaz-Campos, M., et al. Shale gas-in-place calculations Part I: New pore-scale considerations. *SPE Journal*, 2012, 17: 219-229.
- Bharath, R., Carl, T., Ramkumar, S. Simplified local density model for adsorption-over large pressure ranges. *AIChE Journal*, 1995, 41(4): 838-845.
- Brunauer, S., Emmett, P.H., Teller, E., et al. Adsorption of gases in multimolecular layers. *Journal of the American Chemical Society*, 1938, 60: 309-319.
- Cai, J., Tian, Z., Zhou, S., et al. Controlling factor analysis of microstructural property and storage capacity of deep Longmaxi Formation shale in Sichuan Basin. *Energy & Fuels*, 2021, 35(24): 20092-20102.
- Chalmers, G. R., Bustin, R. M., Power, I. M. Characterization of gas shale pore systems by porosimetry, pycnometry, surface area, and field emission scanning electron microscopy/transmission electron microscopy image analyses: Examples from the Barnett, Woodford, Haynesville, Marcellus, and Doig units. *AAPG Bulletin*. 2012, 96: 1099-1119.
- Chen, M., Kang, Y., Zhang, T., et al. Methane adsorption behavior on shale matrix at in-situ pressure and temperature conditions: Measurement and modeling. *Fuel*, 2018, 228: 39-49.
- Cochran, T. W., Kabel, R. L., Danner, R. P. Vacancy solution theory of adsorption using Flory-Huggins activity coefficient equations. *AIChE Journal*, 1985, 31(2): 268-277.
- Curtis, J. B. Fractured shale-gas systems. *AAPG Bulletin*, 2002, 86: 1921-1938.
- Dong, D., Shi, Z., Guang, Q., et al. Progress, challenges and prospects of shale gas exploration in the Wufeng-Longmaxi reservoirs in the Sichuan Basin. *Natural Gas Industry*, 2018, 38(4): 67-76. (in Chinese)
- Donohue, M. D., Aranovich, G. L. A New classification of isotherms for Gibbs adsorption of gases on solids. *Fluid Phase Equilibria*, 1999, 158-160: 557-563.
- Duan, X., Hu, Z., Gao, S., et al. Shale high pressure isothermal adsorption curve and the production dynamic experiments of gas well. *Petroleum Exploration and Development*, 2018, 45(1): 127-135.
- Dubinina, M. M., Stoeckli, F. Homogeneous and heterogeneous micropore structures in carbonaceous adsorbents. *Journal of Colloid and Interface Science*, 1980, 75(1): 34-42.
- Fianu, J., Gholinezhad, J., Hassan, M. Comparison of temperature-dependent gas adsorption models and their application to shale gas reservoirs. *Energy & Fuels*, 2018, 32(4): 4763-4771.
- Gasparik, M., Bertier, P., Gensterblum, Y., et al. Geological controls on the methane storage capacity in organic-rich shales. *International Journal of Coal Geology*, 2014, 123: 34-51.
- Gasparik, M., Ghanizadeh, A., Gensterblum, Y., et al. Multi-temperature method for high-pressure sorption measurements on moist shales. *Review of Scientific Instruments*, 2013, 84(8): 085116.
- Hartman, R. C., Ambrose, R. J., Akkutlu, I. Y., et al. Shale gas-in-place calculations part II-multi-component gas adsorption effects. Paper SPE 144097 Presented at North American Unconventional Gas Conference and Exhibition, The Woodlands, Texas, 14-16 June, 2011.
- Huston, N. D., Yang, R. T. Theoretical basis for the Dubinin-Radushkevich (DR) adsorption isotherm equation. *Adsorption*, 1997, 3(3): 189-195.
- Li, A., Han, W., Fang, Q., et al. Experimental investigation of methane adsorption and desorption in water-bearing shale. *Advances in Geo-Energy Research*, 2020, 3(3): 45-55.
- Li, J., Li, B., Gao, Z., et al. Adsorption behavior, including the thermodynamic characteristics of wet shales under different temperatures and pressures. *Chemical Engineering Science*, 2021, 230: 116228.
- Li, W., Li, J., Lu, S., et al. Evaluation of gas-in-place content and gas-adsorbed ratio using carbon isotope fractionation model: A case study from Longmaxi shales in Sichuan Basin, China. *International Journal of Coal Geology*, 2022, 249: 103881.
- Liu, D., Yao, Y., Chang, Y. Measurement of adsorption phase densities with respect to different pressure: Potential application for determination of free and adsorbed methane in coalbed methane reservoir. *Chemical Engineering Journal*, 2022, 446(3): 137103.
- Ma, X., Xie, J., Yong, R., et al. Geological characteristics and high production control factors of shale gas reservoirs in Silurian Longmaxi Formation, Southern Sichuan Basin, SW China. *Petroleum Exploration and Development*, 2020, 47(5): 901-915.
- Ma, X., Wang, H., Zhou, S., et al. Deep shale gas in China: Geological characteristics and development strategies. *Energy Reports*, 2021, 7: 1903-1914.
- Mengal, S. A., Wattenbarger, R. A. Accounting for adsorbed gas in shale gas reservoirs. Paper SPE 141085 Presented at SPE Middle East Oil and Gas Show and Conference, Manama, Bahrain, 25-28 September, 2011.
- Ono, S., Kondo, S. Molecular theory of surface tension in liquids, in *Structure of Liquids/Struktur der Flüssigkeiten*, edited by Green H. S., et al., Springer, Berlin, Heidelberg, pp. 134-280, 1960.
- Pan, Z., Connell, L. D. Reservoir simulation of free and adsorbed gas production from shale. *Journal of Natural Gas Science and Engineering*, 2015, 22: 359-370.
- Pang, W., Jin, Z. Revisiting methane absolute adsorption in organic nanopores from molecular simulation and Ono-Kondo lattice model. *Fuel*, 2019, 235: 339-349.
- Peter, J. C., Tim, A. M., Tennille, E. M. Influence of moisture content and temperature on methane adsorption isotherm analysis for coals from a low-rank, biogenically sourced gas reservoir. *International Journal of Coal Geology*, 2008, 76(1-2): 166-174.
- Polanyi, M. The potential theory of adsorption. *Science*, 1963, 141(3585): 1010-1013.
- Qin, X., Harpreet, S., Cai, J. Sorption characteristics in coal and shale: A review for enhanced methane recovery. *Capillarity*, 2022, 5(1): 1-11.
- Rexer, T. F., Mathia, E. J., Aplin, A. C., et al. High-pressure

- methane adsorption and characterization of pores in Posidonia Shales and Isolated Kerogens. *Energy & Fuels*, 2014, 28(5): 2886-2901.
- Ross, D. J. K., Bustin, R. M. The importance of shale composition and pore structure upon gas storage potential of shale gas reservoirs. *Marine and Petroleum Geology*, 2009, 26(6): 916-927.
- Sakurovs, R., Day, S., Weir, S., et al. Application of a modified Dubinin-Radushkevich equation to adsorption of gases by coals under supercritical conditions. *Energy & Fuels*, 2007, 21(2): 992-997.
- Sing, K. Adsorption methods for the characterization of porous materials. *Advances in Colloid and Interface Science*, 1998, 76(77): 3-11.
- Wang, Z., Li, Y., Guo, P., et al. Analyzing the adaption of different adsorption models for describing the shale gas adsorption law. *Chemical Engineering and Technology*, 2016, 39(10): 1921-1932.
- Wu, K., Li, X., Wang, C., et al. A model for surface diffusion of adsorbed gas in nanopores of shale gas reservoirs. Paper OTC 25662 Presented at Offshore Technology Conference, Houston, Texas, 4-7 May, 2015.
- Wu, T., Zhao, H., Tesson, S., et al. Absolute adsorption of light hydrocarbons and carbon dioxide in shale rock and isolated kerogen. *Fuel*, 2019, 235: 855-867.
- Xiang, Z., Liang, H., Qi, Z., et al. Mathematical model for isothermal adsorption of supercritical shale gas. *Journal of Porous Media*, 2019, 22(4): 499-510.
- Xiong, J., Liu, X., Liang, L., et al. Adsorption of methane in organic-rich shale nanopores: An experimental and molecular simulation study. *Fuel*, 2017, 200: 299-315.
- Xue, H., Wang, H., Liu, H., et al. Absorptivity capacity and aperture distribution characteristics of shales taking the Longmaxi Formation Shale of Sichuan Basin as an example. *Acta Physica Sinica*. 2013, 34(5): 826-832. (in Chinese)
- Yang, Y., Liu, S., Clarkson, C. Quantification of temperature dependent sorption isotherms in shale gas reservoirs: Experiment and theory. Paper SPE 205897 Presented at SPE Annual Technical Conference and Exhibition, Dubai, UAE, 21-23 September, 2021.
- Yu, W., Sepehrnoori, K., Patzek, T. W. Modeling gas adsorption in marcellus shale with Langmuir and BET Isotherms. *SPE Journal*, 2016, 21(2): 589-600.
- Zhang, T., Ellis, G., Ruppel, S. C., et al. Effect of organic matter type and thermal maturity on methane adsorption in shale gas systems. *Organic Geochemistry*, 2012, 47: 120-131.
- Zhang, C., Zhang, J., Li, W., et al. Deep shale reservoir characteristics and exploration potential of Wufeng-Longmaxi Formations in Dazu area, western Chongqing. *Nature Gas Geoscience*, 2019, 30(12): 1794-1804. (in Chinese)
- Zhou, S., Ning, Y., Wang, H., et al. Investigation of methane adsorption mechanism on Longmaxi shale by combining the micropore filling and monolayer coverage theories. *Advances in Geo-Energy Research*, 2018, 2(3): 269-281.
- Zhou, S., Liu, H., Chen, H., et al. A comparative study of the nanopore structure characteristics of coals and Longmaxi Shales in China. *Energy Science and Engineering*, 2019, 7(6), 2768-2781.
- Zhu, L., Zhang, C., Zhang, Z., et al. High-precision calculation of gas saturation in organic shale pores using an intelligent fusion algorithm and a multi-mineral model. *Advances in Geo-Energy Research*, 2020, 4(2): 135-151.
- Zou, C., Zhao, Q., Cong, L., et al. Development progress, potential and prospect of shale gas in China. *Natural Gas Industry*, 2021, 41(1): 1-14. (in Chinese)